THE NEW DRIFT CHAMBER FOR THE MARK II DETECTOR AT THE SLAC LINEAR COLLIDER*

PATRICIA R. BURCHAT, GAIL G. HANSON, HARTMUT F.-W. SADROZINSKI[†]

Stanford Linear Accelerator Center, Stanford, California, 94305

Abstract

The design of the new cylindrical drift chamber for the Mark II detector at the SLAC Linear Collider is described. Prototype tests to determine the working parameters of the chamber and to study possible gas mixtures are discussed.

1. Introduction

The first detector to study Z^0 physics at the SLAC Linear Collider (SLC)[1] will be an upgrade[2] of the Mark II detector[3] which has run successfully at both the SPEAR and PEP e^+e^- storage rings at SLAC. With the existing Mark II drift chamber, precision for high momentum tracks is limited by the relatively small number of layers. Pattern recognition capability is limited by the inability to record more than one hit per sense wire. Consequently, a new cylindrical drift chamber is being constructed for SLC. It will provide good momentum resolution with the Mark II 5 kG magnet, good solid angle coverage, and multi-hit capability for ease of pattern recognition and high tracking efficiency. In addition, the new drift chamber will measure charged particle energy loss due to ionization (dE/dx) as an independent aid to calorimetry in electron-hadron separation for particle momenta less than about 10 GeV/c. The design and construction of the new chamber and prototype tests will be discussed.

2. Design and Construction

2.1 CELL DESIGN

The design of the new drift chamber is based on a cell containing six sense wires staggered ±380 μm from the cell axis to provide local left-right ambiguity resolution. Figure 1 shows the basic dimensions of the cell. The 30 μm diameter sense wires are spaced 8.33 mm apart. There are two guard wires at each end of the cell for shaping the electric field and equalizing the gain of all the sense wires. Potential wires are placed between the sense wires to reduce crosstalk between sense wires, to reduce electrostatic deflection of the sense wires, and to allow control of the gain of the sense wires and the electric field in the cell independently. There are nineteen field wires in each cell. The average cell half-width is 3.3 cm.

The cell just described has a very uniform electric drift field across the cell resulting in uniform dE/dx sampling regions and a simple time-distance relation. This uniformity can be seen in Figure 2 which shows the drift trajectories of electrons.

2.2 CHAMBER DESIGN

The cells are arranged in 12 concentric layers with a minimum radial distance of 2.5 cm between layers. This results in 5832 sense wires and 72 drift-time and dE/dx measurements per track. Alternate layers have their wires parallel to the axis or at ±3.8° to the axis to provide stereo information.

DRIFT CHAMBER WIRE PATTERN

× Sense Wire   ○ Guard Wire
• Potential Wire   ● Field Wire

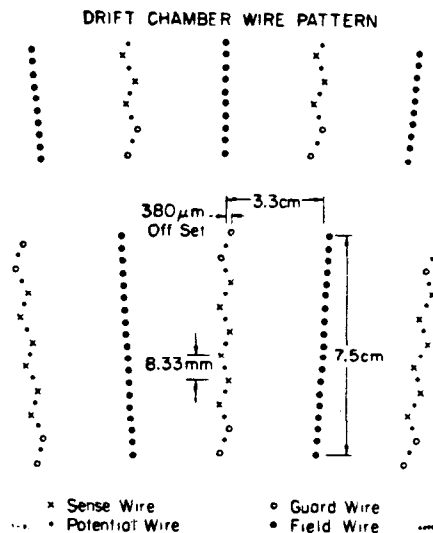Fig. 1. Drift chamber cell configuration.

The active volume of the chamber has a length of 2.30 m and inner and outer radii of 19.2 cm and 151.9 cm respectively. The 36,936 wires are strung between two-inch thick aluminum endplates which are prestrained to maintain uniform wire tension during stringing.

2.3 FEEDTHROUGH DESIGN

The nineteen wires in one row of a cell are positioned by a single injection-molded Delrin 500AF feedthrough. These wires are located in machined notches along one side of a slot in the feedthrough. The notches are machined at the same time as three pin-holes which accurately locate the feedthrough on the endplate. The single open slot in the feedthrough allows nineteen wires to be strung at once and allows access for wire replacement, if necessary, and visual inspection of the interior.

3. Prototype and Gas Studies

Two prototypes were built to study the characteristics of the cell design and to study possible gas mixtures to be used in the new drift chamber. In particular, we studied gases composed of argon, methane and CO_2 in various proportions. The primary motivation for studying these gases was to search for a gas with a low electron drift velocity as well as good position, double track and dE/dx resolution and stability against breakdown. A mixture of 50% argon - 50% ethane was also studied.

The advantages of a gas with low electron drift velocity fall into three categories as listed below.

1. Effects depending on the temporal characteristics of the pulses are scaled by the drift velocity when their influence on the position resolution and double track resolution is evaluated.

   (a) The contribution of the 1/t tail to the multiple track separation is reduced in proportion to the electron drift velocity.

Presented at the Nuclear Science Symposium, Orlando, Florida, October 31 – November 2, 1984.

(b) Effects of rise time, time slewing and time walk are reduced in proportion to the drift velocity.

(c) Slower, more reliable clock speeds can be used in the TDC system and differential non-linearities in the TDC system are less significant for a low drift velocity.

2. The Lorentz angle (the angle between the electric field lines and the electron drift trajectories) depends linearly on the electron drift velocity.

3. The gases with low electron drift velocity which we tested tended to be saturated with the slope of the drift velocity versus electric field being negative. This is advantageous for the following reason. The electrons with the longest drift trajectory are those which pass closest to the potential wires. The electric field is lower in this region. An increasing drift velocity with decreasing electric field will partially compensate for the longer drift path. This provides a focusing effect which makes the pulse narrower.
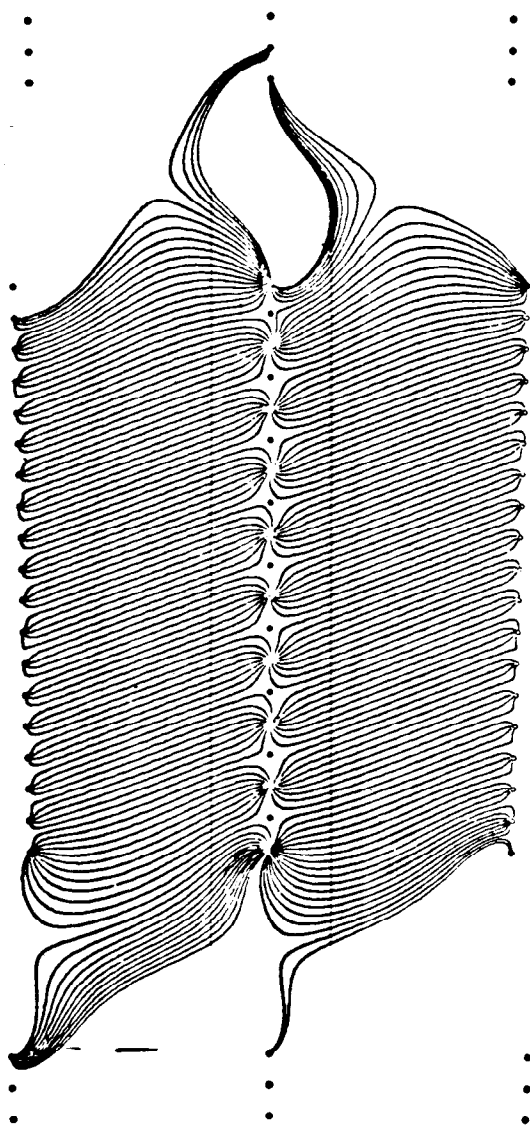

Fig. 2. Electron drift trajectories in drift chamber cell.

3.1 ELECTRON DRIFT VELOCITY

Figure 3 shows the electron drift velocity as a function of drift field for four of the gases considered. These curves are the results of measurements made using a small drift chamber constructed for this purpose.
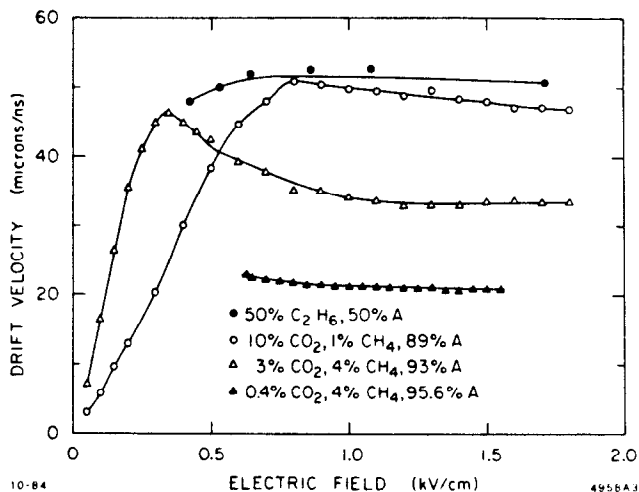

Fig. 3. Electron drift velocity versus electric field.

The four representative gases are:

1. 10% CO_2, 1% methane, 89% argon which will be referred to as HRS gas[4] and has an electron drift velocity of about 50 $\mu m/ns$ at the drift field in most of the cell;

2. 50% argon, 50% ethane which was used in the old Mark II drift chamber and has a drift velocity of 52 $\mu m/ns$;

3. 3% CO_2, 4% methane, 93% argon which has a drift velocity of 33 $\mu m/ns$;

4. 0.4% CO_2, 4% methane, 95.6% argon which has a drift velocity of 21 $\mu m/ns$.

3.2 POSITION RESOLUTION

The position resolution was measured with a one-cell, full-length prototype using a LeCroy 2228A · 8 channel TDC with 1 ns bin width. For each gas, cosmic ray data was recorded and analysed for at least two different sense wire gains. The data was binned in 2 mm wide bins in x where x is the distance between the track and the sense wire. The position resolution was measured as a function of x by averaging the variance of the distribution of residuals of two triplets of wires. The resolution was measured separately for tracks passing to the left and right of the sense wire plane.

It was assumed that $\sigma_w^2 = \sigma_d^2 + \sigma_0^2$, where σ_w is the total resolution for an individual wire, σ_d is the resolution due to x dependent effects, and σ_0 is the resolution with no x dependence. We then assumed that this x dependence is a result of diffusion, i.e., $\sigma_d = D\sqrt{x}$, where D is an effective diffusion coefficient. A least squares line fit was made to σ_w^2 versus x to determine D and σ_0 for each gas. These parameters were used to calculate the average resolution across the cell, $\langle \sigma \rangle$, for each gas.

Figure 4 shows the measured position resolution as a function of x for the four representative gases. The resolution corresponding to the fit to these data is also shown. D, σ_0 and $\langle \sigma \rangle$ are shown in Table 1. The effective diffusion coefficients, D, range from 73 $\mu m/\sqrt{cm}$ to 144 $\mu m/\sqrt{cm}$ and are thus a factor

2

of 2 or 3 smaller than the longitudinal diffusion coefficient for single electrons.[5] The ratio is a statistical factor which depends on the number of primary electrons collected and the number of primary electrons necessary to trigger the discriminator.
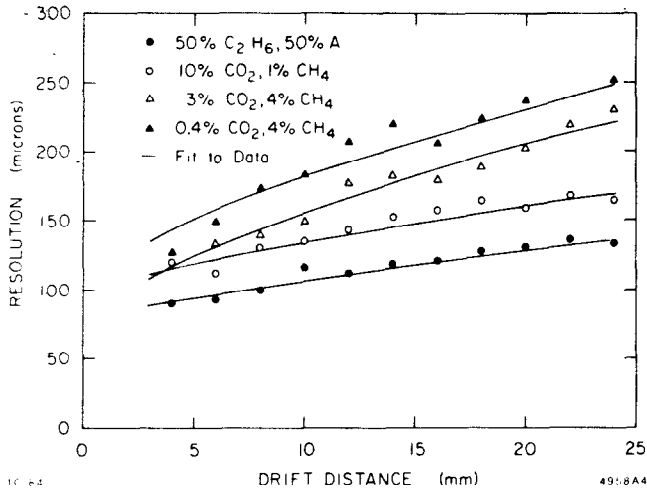

Fig. 4. Position resolution versus drift distance.

Table 1
POSITION RESOLUTION
for ⟨ pulse height ⟩ = 3.0 mV at preamp input

Gas Composition %			σ_0 (μm)	D ($\mu m/\sqrt{cm}$)	$\langle \sigma \rangle$ (μm)
CO_2	methane	argon	±5 μm	±4 $\mu m/\sqrt{cm}$	±6 μm
10.0	1.0	89.0	100	90	153
3.0	4.0	93.0	80	134	189
0.4	4.0	95.6	111	144	216
50% ethane, 50% argon			79	73	123

In Figure 5, ⟨σ⟩ is plotted as a function of percent argon for all the gases studied. We observe that gases with large amounts of argon generally have poorer resolution mainly due to the large diffusion contributions.
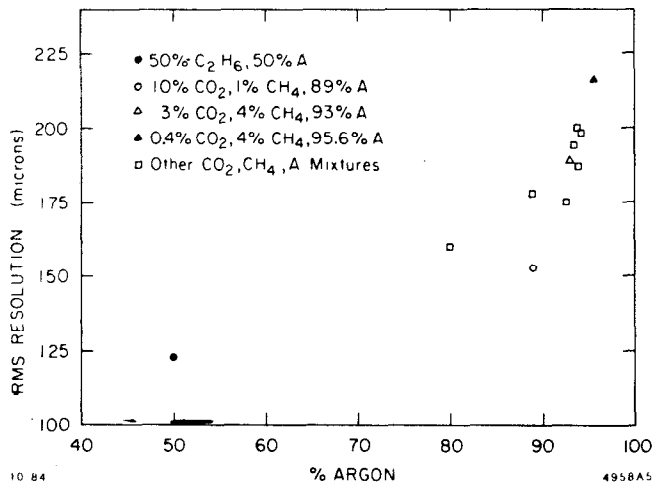

Fig. 5. Position resolution for average drift distance versus percentage of argon in the gas.

The resolution for 50% argon - 50% ethane is about 75% that of HRS gas.

Some of the contributions to the resolution are:

Electronics Resolution: The RMS resolution due to the 1 ns timing bins for the TDC is $(1\ ns/\sqrt{12})v_d \approx 15\ \mu m$ for an electron drift velocity, v_d, of 50 $\mu m/ns$. That due to noise is $(\sigma_{noise}/V_{peak})\tau_{rise}v_d \approx 10\ \mu m$.

Rise Time: Maximum changes in timing due to walk are $(V_{thres}/V_{peak})\tau_{rise}v_d \approx 40\ \mu m$.

Diffusion: Besides the z-dependent diffusion contribution to the resolution, there is a constant contribution from the high field region around the wire.[6] This effect increases the parameter defined as σ_0. The contribution can be large ($\approx$ 50 μm) and is gas dependent.

Collection: Cluster statistics and non-uniform collection across the cell can be a large contribution with a dependence on the saturation of the drift velocity.

3.3 MULTIPLE TRACK SEPARATION

The spatial width of the pulse from the chamber determines how far apart in space two tracks must be before they can be resolved. For double track separation using the TDC, the first pulse must fall below the discriminator threshold before the arrival of the second pulse. The main contribution to the pulse width comes from the distribution of drift times for the collected electrons. To first order, the spatial pulse width is equal to half the separation between sense wires which is 4.17 mm in this cell. The pulse width can also be affected by the following factors.

- The variation of drift velocity with decreasing electric field will determine whether there is a focusing or defocusing effect for electrons which drift close to the potential wires (see above).

- The contribution of the $1/t$ tail to the spatial width is proportional to the drift velocity.

- Large diffusion coefficients result in broader pulses.

The temporal width of the pulse at the TDC discriminator threshold was measured. For each gas, the mean time over threshold was multiplied by the drift velocity to determine the spatial separation needed to resolve two tracks. Figure 6 shows the spatial pulse width as a function of electron drift velocity for the four gases.
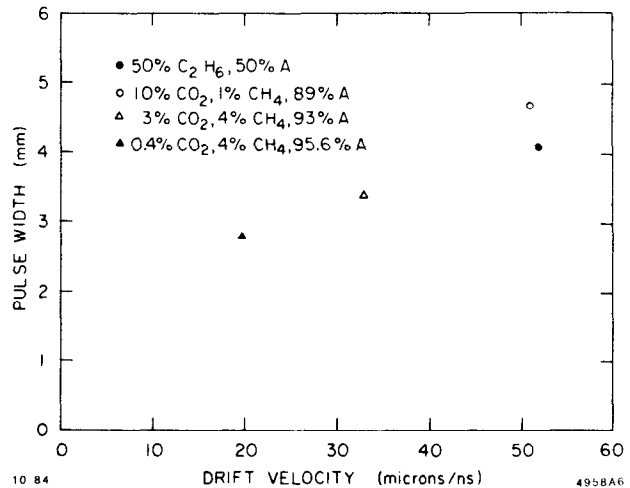

Fig. 6. Pulse width versus drift velocity.

The 4% methane, 3% CO_2 mixture and the 4.0% methane, 0.4% CO_2 mixture have good focusing properties (increasing drift velocity with decreasing electric field) and thus have small pulse widths. This is the dominant effect. The pulse width is also correlated with the drift velocity (because of the $1/t$ tail) and the magnitude of the diffusion coefficient but these effects are not as significant.

Note that these measurements represent the pulse width at the TDC threshold. With a sampling dE/dx system, the minimum separable distance between double tracks could be reduced by nearly a factor of two.[7]

3.4 GAIN

The gain of the chamber depends on both the charge per unit length on the sense wire and the amount of argon in the gas. The relative gains of different gas/high-voltage configurations were measured. Figure 7 shows the charge on the sense wire which yields a mean pulse height of 3 mV at the preamp input for five gases. The position resolution measurements shown in Figures 4 and 5 and the pulse width measurements shown in Figure 6 correspond to this gain.
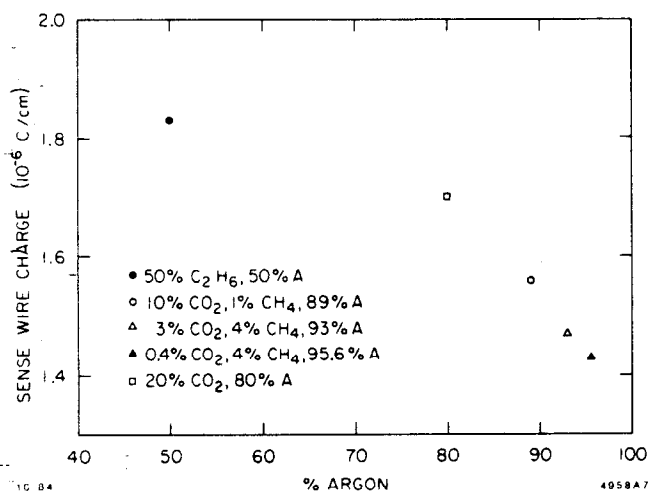

Fig. 7. Charge per unit length on sense wires for equal pulse height as a function of percentage of argon in the gas.

Since the gas with the lowest drift velocity (4% methane, 0.4% CO_2) contains more argon than any other gas tested, it does not need as much charge on the sense wires to produce the same gain as the other gases. The argon-ethane mixture, which contains only 50% argon, requires 16% more charge on the sense wire to produce the same gain as HRS gas. Consequently, the voltage on the field and potential wires must be higher.

3.5 dE/dx RESOLUTION

To measure dE/dx resolution a 50-cm-long chamber consisting of three layers of three cells each was operated in a 10 GeV positron beam. By combining events to get 72 dE/dx measurements and discarding the 24 highest pulses (corresponding to the largest fluctuations on the Landau tail), we measure the following dE/dx resolution: $\sigma_{dE/dx} = 5.7\%$ for HRS gas and $\sigma_{dE/dx} = 4.7\%$ for 3% CO_2, 4% methane, 93% argon. The dE/dx resolution we actually obtain with the new drift chamber will depend on our ability to correct for systematic changes in gain due to saturation, stereo layers crossing axial layers, temperature and atmospheric pressure changes, etc.

3.6 GAS STABILITY

All gases being considered were tested for stability against breakdown.

Stability tests for HRS gas were done with a single wire strung in a 3/4 inch diameter tube. The diameter of the wire was varied and the tube was operated with the wire acting either as an anode or a cathode. The electric field on the surface of the wire when breakdown of the gas occurred is shown in Table 2 for different wire diameters. Note that the gas around a sense wire generally breaks down at a higher voltage than around a field wire of the same diameter. The wire diameters and maximum surface fields for the new Mark II drift chamber are 30 μm and -187 kV/cm for the sense wires, 100 μm and -76 kV/cm for the guard wires, 178 μm and 21 kV/cm for the field wires, and 304 μm and 20 kV/cm for the end field wires. However, the charges on the wire at breakdown given in Table 2 cannot be used as limits for safe running in the final chamber since feedback between sense and field wires with gain results in a lower breakdown threshold.

Table 2
GAS STABILITY
Electric field on surface of wire
in 3/4 inch tube at breakdown in HRS gas.

Field Wire diameter (μm)	E_f (kV/cm)	Sense Wire diameter (μm)	E_s (kV/cm)
20	190	20	280
30	147	30	220
50	118	50	154
100	83	100	98
177	69	177	70
305	54		

In order to study this feedback effect, a small chamber with a replaceable sense wire and four 175 μm field wires was constructed. Negative voltage was applied to the field wires and the sense wire was connected to ground. The conducting chamber walls were connected to ground or negative voltage in order to control the charge on the sense and field wires independently. The diameter of the sense wire was varied between 20 μm and 175 μm.

It was found that breakdown occurred in HRS gas when the total gain from sense and field wires[8] is about 10^7. This effect is shown in Fig. 8 where the gain of the field wires is plotted against the gain of the sense wire at breakdown.

Needles of hydrocarbon polymers formed on the field wires when the amount of methane in the gas was greater than $\approx 5\%$ almost independent of the amount of CO_2. The 50% argon - 50% ethane mixture behaved very differently. The voltage could initially be raised quite high before current was drawn. But then the gas polymerized rapidly around the field wires and breakdown occurred at much lower voltages.

3.7 SUMMARY OF GAS STUDIES

We conclude that of the gases tested, those most suitable for use in the Mark II drift chamber at SLC are HRS gas ($v_d = 50$ $\mu m/ns$, $\langle \sigma \rangle = 153$ μm, pulse width = 4.7 mm, $\sigma_{dE/dx} = 5.7\%$) and 3% CO_2, 4% methane, 93% argon ($v_d = 33$ $\mu m/ns$, $\langle \sigma \rangle = 189$ μm, pulse width = 3.4 mm, $\sigma_{dE/dx} = 4.7\%$). The

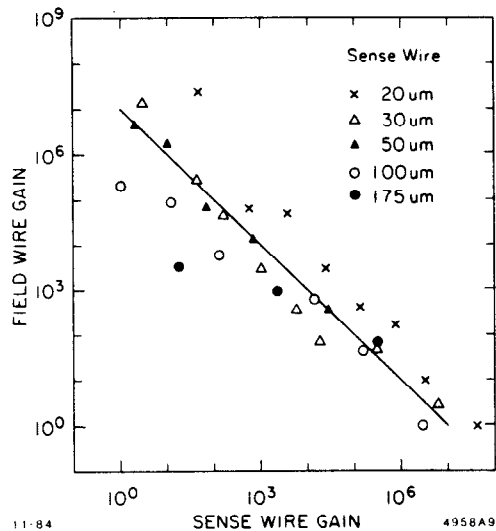50% argon, 50% ethane mixture will not be used because of gas breakdown problems.

Fig. 8. Gain of the field wire versus gain of the sense wire at breakdown for HRS gas. The solid line represents a combined gain of 10^7.

4. Conclusion

The chamber is presently being strung at a rate of $\approx$ 3000 wires per week with completion of stringing expected in early December, 1984. The upgraded detector will be moved into the interaction region at PEP for checkout. The data taken at PEP will be used for final development of tracking programs and algorithms for dE/dx measurements before the move to SLC beginning in January, 1986.

Acknowledgements

References

1. SLAC Linear Collider Conceptual Design Report, SLAC-229, June, 1980.

2. Proposal for the Mark II at SLC, CALT-68-1015, April, 1983.

3. R.H.Schindler, et al.,Phys. Rev. D 24, 78 (1981).

4. This mixture has been used successfully in the High Resolution Spectrometer at PEP and the Mark III detector at SPEAR.

5. F.Piuz, NIM 205 (1983), 425.

6. Dimethylether: A Low Veolcity, Low Diffusion Drift Chamber Gas, F. Villa, SLAC-PUB-3037, January, 1983.

7. Review of dE/dx System for Mark II/SLC, Mark II/SLC Note 45.

8. Principles of Operation of Multiwire Proportional and Drift Chambers, F. Sauli, CERN-77-09, May, 1977, pp. 35-44.